Iranian Journal of Pharmaceutical Sciences
2025: 21 (1): 430- 447
https://journals.sbmu.ac.ir/IJPS

Research Article

OPEN ACCESS

Exploration of Chalcones as Antimicrobial agents: Synthesis, Characterization, Antimicrobial Evaluation and Molecular Docking studies

Kanaka Raju Addipalli [a*], Rajendra Prasad Yejella [b], Girija Sastry Vedula [c]

[a] *Research Scholar, Pharmaceutical Chemistry division, A.U. College of Pharmaceutical Sciences, Andhra University, Visakhapatnam 530003, Andhra Pradesh, India.*

[b] *Pharmaceutical Chemistry division, Vignan Institute of Pharmaceutical Technology, Duvvada, Visakhapatnam-530049, Andhra Pradesh, India.*

[c] *Pharmaceutical Chemistry Division, A.U. College of Pharmaceutical Sciences, Andhra University, Visakhapatnam 530003, Andhra Pradesh, India.*

Received: December 6, 2024 **Last Revision:** February 3, 2025 **Accepted:** July 21, 2025 **Available online:** December 21, 2025.

Abstract

Although many medications are available to treat infectious infections, their therapeutic efficacy is hampered by systemic toxicities, drug resistance, hypersensitivity, and a narrow antibacterial spectrum. Based on the above facts, we synthesized and evaluated some new chalcones' antibacterial and antifungal properties. A group of natural compounds called chalcones has a broad spectrum of biological activity. The Claisen-Schmidt condensation of 4-tert-butyl-2,6-dimethyl-3,5-dinitro acetophenone with a variety of substituted aromatic and heteroaromatic aldehydes yielded some new chalcones with different substituents in consideration of the wide range of biological activities related to chalcones. Column chromatography and recrystallization techniques were used to purify the produced chalcones. IR, ^{1}H NMR, and elemental analysis data characterized the purified chalcones. These substances underwent additional testing for antimicrobial activity using the serial tube dilution technique. Antibacterial testing revealed potent activity for chalcones R1, R5, R6, and R18 (MIC: 32 µg/mL), attributed to electron-withdrawing groups like dichloro, nitro, and difluoro substituents. Antifungal studies identified R1, R3, and R18 as the most effective (MIC: 16 µg/mL against *Aspergillus niger* and *Candida tropicalis*), with SAR analysis emphasizing the roles of halogens and methoxy groups in enhancing activity. Quality evaluation of the protein PDB: 4AMV confirmed its suitability for molecular docking studies using the SAVES server and binding pocket analysis using CASTp and BIOVIA Discovery studio. Docking of chalcones against PDB: 4AMV using Auto Dock Vina module of PyRx 0.8 revealed binding affinities ranging from −7.2 to −8.4 kcal/mol, with ciprofloxacin (standard) showing −8.3 kcal/mol. Chalcone R6 exhibited the greatest affinity for binding (-8.4 kcal/mol) and robust interactions, including hydrogen bonds and hydrophobic contacts. R1, R5, and R9 also demonstrated significant affinities (−8.2 to −8.0 kcal/mol). These findings highlight chalcones, particularly R6, as promising candidates for further antimicrobial development.

Keywords: Chalcones; Claisen-Shmidt reaction; Antimicrobial Evaluation; Molecular Docking.

*** Corresponding Author**:

Kanaka Raju Addipalli, Pharmaceutical Chemistry division, Vignan Institute of Pharmaceutical Technology, Duvvada, Visakhapatnam-530049, Andhra Pradesh, India. E-mail: rajuaddipalli81@gmail.com.

Cite this article as: Addipalli K.R., Yejella R.P., Vedula G. S. Exploration of Chalcones as Antimicrobial agents: Synthesis, Characterization, Antimicrobial Evaluation and Molecular Docking studies. Iran. J. Pharm. Sci., 2025, 21 (1): 430- 447.

DOI: https://doi.org/10.22037/ijps.v21i1.46927

1. Introduction

Microorganisms like bacteria, fungi, and viruses are responsible for causing infectious diseases in humans. These conditions are managed with the help of different antimicrobial drugs available on the market. However, the increasing dependence on these medications has raised a significant issue: antimicrobial resistance (AMR) [1, 2]. Antimicrobial resistance seriously threatens public health, leading to a notable increase in illness, death, and hospitalizations. In response to this challenge, the World Health Organization (WHO) launched the slogan "No action today, no cure tomorrow" to address the growing issue of AMR [3–5]. The challenges posed by current antimicrobial agents, such as antimicrobial resistance (AMR), undesirable side effects, prolonged treatment durations, and suboptimal therapeutic outcomes, highlight the need to develop new, more effective antimicrobial compounds that can serve as reliable drugs. Scientists are constantly exploring new antimicrobial agents using various approaches. A widely adopted method involves designing and synthesizing small molecules to evaluate their potential as antimicrobial drug candidates. Small molecule drugs are crucial for treating a variety of diseases. However, their development has slightly declined in recent years, as reported by the United States Food and Drug Administration (US-FDA), with 74% in 2017 and 71% in 2018. In 2019, approximately 70% of all approved targeted drugs were small molecules [6, 7]. Small molecules offer several benefits, including improved pharmacokinetics, oral bioavailability, efficient delivery, and lower production costs [8]. Small molecules provide greater chemical diversity more quickly and conveniently than the processes of isolating, analyzing structures, and testing natural products for biological activity. Furthermore, the pharmaceutical industry commonly uses libraries of synthetic small molecules to screen for lead compounds with promising drug-like characteristics [9].

Chalcones are part of the family of flavonoids and are secondary metabolites found in various edible and medicinal plants. Structurally, they are 1, 3-diphenyl-2-propen-1-ones, featuring two aryl groups connected through an α, β-unsaturated carbonyl system [10]. This system includes a characteristic −C═O–CH═CH– ketoethylenic group, contributing to their delocalized π-electron arrangement in the aromatic rings [11]. Chalcones are primarily polyphenolic compounds, exhibiting vibrant colors ranging from yellow to orange, which play a role in the pigmentation of some plant corollas. Naturally present in fruits, teas, spices, and soy-based foods, chalcones have garnered significant interest for their intriguing chemical properties and potential health benefits. Additionally, these compounds are found in nature as plant allelochemicals, insect hormones, and pheromones [12, 13]. Chalcones are notable for their diverse chemical reactivity and are widely used to produce heterocyclic compounds. They are synthesized by reacting aryl ketones with aromatic aldehydes in the presence of suitable condensing agents [14]. These derivatives serve as critical intermediates in the biosynthesis of flavonoids, isoflavonoids, and aurones [15]. Over the past decades, chalcones have been a focus of medicinal chemistry research due to their broad pharmacological potential. Their reported biological activities include antibacterial [16-18], anti-inflammatory [19-21], analgesic [22, 23], anticholinergic [24], antiplatelet [25], antiulcer [26], antioxidant [27, 28], antimalarial [29], anticancer [30, 31], antiviral [32-35], antileishmanial, [36] antidiabetic [37, 38], immunomodulatory [39, 40], aldose reductase inhibitory [41], estrogenic [42] acetylcholinesterase inhibitory [43] and non-purine xanthine oxidase inhibitory effects [44]. Chalcones are highly appealing in medicinal chemistry due to their straightforward synthesis, structural simplicity, and wide-ranging biological applications.

This study outlines the synthesis of a series of chalcones (R1 to R20) through the reaction of 4-tert-butyl-2, 6-dimethyl-3, 5-dinitroacetophenone with various aromatic and heteroaromatic aldehydes. IR spectroscopy, ^{1}H NMR, and elemental analysis were used to confirm the structures of the synthesized chalcones. Additionally, the AutoDock Vina module in PyRx 0.8 was used for molecular docking investigations, and the serial tube dilution technique was used to assess the antibacterial qualities of the molecules.

2. Materials and methods

2.1. chemicals and instruments

Every chemical employed in this study was of analytical quality and was acquired from a commercial supplier. The spectral-grade organic solvents, including methanol, ethyl acetate, and hexane were utilized without additional purification. Some solvents were bought from Otto Chemie Pvt. Ltd. Mumbai, India, while others were bought from local suppliers. Merck grade precoated TLC

silica gel 60 F254 plates (Merck KGaA, Darmstadt, Germany) were used for TLC chromatography, and the spots were visible under a UV lamp. The Carloerba EA-1108 element analyzer was used for the microanalyses, which came back within ± 0.4% of the theoretical values. We purchased aldehydes, 4-tert-butyl-2, 6-dimethyl-3, 5-dinitro acetophenone from Sigma-Aldrich Chemicals PVT LTD. A digital EZ Melt apparatus (Stanford Research Systems) was utilized to measure the m.p (melting point) in open capillaries; the findings were presented in degrees Celsius without correction. The results are uncorrected and expressed in ◦C. A Bruker ALPHA II FTIR was used to scan the FT-IR spectra, and a Bruker 400 Avance NMR spectrophotometer was used to record the ^{1}HNMR spectra. Tetramethylsilane (TMS) was used as the internal standard, and chemical shifts were represented in δ ppm.

2.2. Synthesis

General Procedure for Synthesis of Chalcones

The series of chalcones (R1 to R20) were prepared (**Scheme 1**) by following the Claisen–Schmidt condensation reaction [45]. Initially, 8 mL of ethanol was used to dissolve one mmol of 4-tert-butyl-2, 6-dimethyl-3, 5-dinitro acetophenone. 4 mL of 30% aqueous sodium hydroxide solution was added dropwise to the previously mentioned solution, which had been agitated on a magnetic stirrer for approximately 6 to 15 hours at room temperature after that one mmol of the appropriate aldehyde had been added. On precoated silica gel-G TLC plates, the progress and completion of the reaction were monitored. Iodine vapors and a UV lamp were used to observe the spots on the plates. Upon the completion of the reaction, the reaction mixture's contents were poured into a beaker of crushed ice. The mixture was then neutralized with 50% hydrochloric acid, allowing the chalcone's crude precipitate to separate. The precipitate was dried in a desiccator after being vacuum-filtered and thoroughly cleaned with cold water. Further, the crude mixture was purified using column chromatography to isolate the pure product. The list of synthesized chalcones (R1 to R20) is listed in **Table 1.**

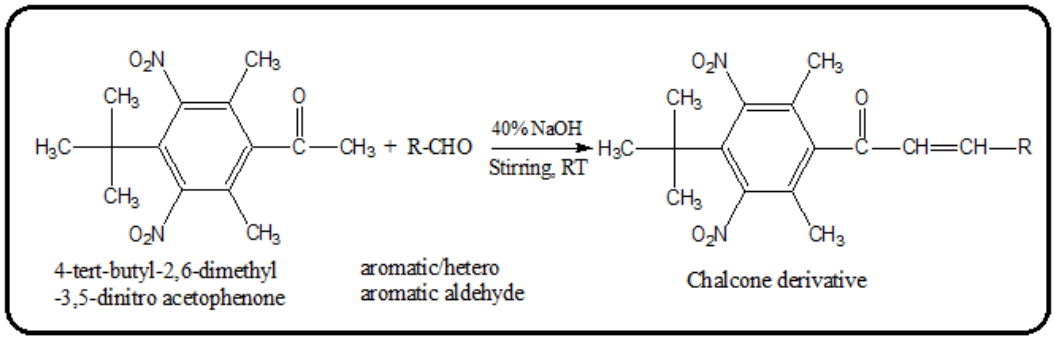

Scheme1. Synthesis of chalcones derivatives using Claisen-Schmidt reaction

Table1. List of synthesized chalcones (R1 to R20)

Compound code	R	Compound code	R
R1	2",4"-dichlorphenyl	R11	4"-fluorophenyl
R2	4"-chlorophenyl	R12	4"-hydroxyphenyl
R3	3",4",5"-trimethoxyphenyl	R13	3",4"-dihydroxyphenyl
R4	4"-dimethylaminophenyl	R14	3"-ethoxy-4"- hydroxyphenyl
R5	3"-nitrophenyl	R15	2"-pyrrolyl
R6	4"-nitrophenyl	R16	2"-thienyl
R7	3"-bromophenyl	R17	4"-methylphenyl
R8	4"-bromophenyl	R18	2",4"-difluorophenyl
R9	3",4"-methylendioxyphenyl	R19	3",4"-dimethoxyphenyl
R10	4"-methoxyphenyl	R20	4"-pyridinyl

R1:Synthesis of (E)-1-(4'-tert-butyl-2', 6'-dimethyl-3',5'-dinitrophenyl)-3-(2",4"- dichlorophenyl)-2-propen-1-one: Yield: 85%; m.w:451g ,m.p:161°C; R_f = 0.6 (20% Ethyl acetate in Hexane); FT-IR (KBr,cm^{-1}): 1651 (C=O), 1622 (C=C Ar), 1583 (CH=CH), 3089 (Ar C-H stretching), 2925 (Alkyl C-H stretching),1534(NO_2), 864 (C-Cl); ^{1}H NMR (400 MHz, $CDCl_3$, ppm), δ: 6.909 (1H, d, J = 16Hz CO-CH=), 7.704 (1H, d, J = 16Hz, Ar-CH=), 1.497 (9H, s, tert-butyl),2.137 (6H, s, Ar-CH_3), 7.285–7.625 (3H,m,C-3'',5'',6''Ar-H), Elm. Anal. Calcd.for $C_{21}H_{20}Cl_2N_2O_5$: C, 55.89%; H, 4.47%; O, 17.73%. Found: C, 55%; H, 4.2%; O, 17%.

R2:Synthesis of (E)-1-(4'-tert-butyl-2',6'-dimethyl-3',5'-dinitrophenyl)-3-(4"- chlorophenyl)-2-propen-1-one : Yield: 75%; m.w:416g, m.p:153°C ; R_f = 0.5 (20% Ethyl acetate in Hexane); FT-IR (KBr,cm^{-1}): 1687 (C=O), 1627 (C=C Ar), 1591 (CH=CH), 1205 (Ar C-H), 2972 (Alkyl C-H stretching),1530 (NO_2), 841 (C-Cl); ^{1}H NMR (400 MHz, $CDCl_3$, ppm), δ: 6.953 (1H, d, J = 16Hz CO-CH=), 7.261(1H, d, J = 16Hz, Ar-CH=), 1.504 (9H,s,tert-butyl), 2.120 (6H,s,Ar-CH_3), 7.447 (2H,d, C-2", 6" Ar-H),7.549 (2H, d, C-3", 5" Ar-H), Elm. Anal. Calcd.for $C_{21}H_{21}ClN_2O_5$: C, 60.51%; H, 5.08%; O, 19.19%. Found: C, 60%; H, 5%; O, 19.2%.

R3: Synthesis of (E)-1-(4'-tert-butyl-2',6'-dimethyl-3',5'-dinitrophenyl)-3- (3",4",5"- trimethoxy phenyl) -2-propen-1-one : Yield: 70%; m.w:472g, m.p:154°C; R_f = 0.7 (20% Ethyl acetate in Hexane); FT-IR (KBr,cm^{-1}): 1651 (C=O), 1619 (C=C Ar), 1579 (CH=CH), 1030 (Ar C-H), 2927 (Alkyl C-H stretching), 1538 (NO_2), 1242 (Ar OCH_3); ^{1}H NMR (400 MHz, $CDCl_3$, ppm), δ: 6.901(1H, d, J = 16Hz CO-CH=), 7.200 (1H, d, J = 16Hz, Ar-CH=), 1.509 (9H, s, tert-butyl), 2.130 (6H, s, Ar-CH_3), 3.929 (9H, s, OCH_3) 7.285 (2H, s, C-2",6" Ar-H). Elm. Anal. Calcd.for $C_{24}H_{28}N_2O_8$: C, 61.01%; H, 5.97%; O, 27.09%. Found: C, 61%; H, 5.2%; O, 27%.

R4:Synthesis of (E)-1-(4'-tert-butyl-2',6'-dimethyl-3',5'-dinitrophenyl)-3-(4"-N,N- dimethylamino phenyl)-2-propen-1-one: Yield: 65%; m.w:425g, m.p.146°C ; R_f = 0.6 (20% Ethyl acetate in Hexane); FT-IR (KBr,cm^{-1}): 1706 (C=O), 1652 (C=C Ar), 1609 (CH=CH), 1021 (Ar C-H), 2923 (Alkyl C-H stretching),1528 (NO_2), 1180 (-N-CH_3); ^{1}H NMR (400 MHz, $CDCl_3$, ppm), δ: 6.781(1H, d, J = 16Hz CO-CH=), 7.200 (1H, d, J = 16Hz, Ar-CH=), 1.500 (9H, s, tert-butyl), 2.132 (6H, s, Ar-CH_3),3.090 (6H, s, N-CH_3),7.490 (2H, d,C-2",6" Ar-H), 6.706 (2H,d,C-3",5" Ar-H). Elm. Anal. Calcd.for $C_{23}H_{27}N_3O_5$: C, 64.93%; H, 6.40%; O, 18.8%. Found: C, 64%; H, 6.2%; O, 18%.

R5:Synthesis of (E)-1-(4'-tert-butyl-2',6'-dimethyl-3',5'-dinitrophenyl)-3-(3"- nitrophenyl)-2-propen-1-one: Yield: 75%; m.w:427g, m.p.175°C; R_f = 0.6 (20% Ethyl acetate in Hexane); FT-IR (KBr,cm^{-1}): 1711 (C=O), 1618 (C=C Ar), 1579 (CH=CH), 1030 (Ar C-H), 2926 (Alkyl C-H stretching),1538 (NO_2); ^{1}H NMR (400 MHz, $CDCl_3$, ppm), δ: 6.972 (1H, d, J = 16Hz CO-CH=), 7.238 (1H, d, J = 16Hz, Ar-CH=), 1.507 (9H, s, tert-butyl), 2.119 (6H,s,Ar-CH_3), 7.286–7.745 (4H, m, C- 2'', 4'', 5", 6'', Ar-H), Elm. Anal. Calcd.for $C_{21}H_{21}N_3O_7$: C, 59.01%; H, 4.95%; O, 26.20%. Found: C, 59%; H, 4.7%; O, 26%.

R6:Synthesis of (E)-1-(4'-tert-butyl-2',6'-dimethyl-3',5'-dinitrophenyl)-3-(4"- nitrophenyl)-2-propen-1-one: Yield: 65%;%; m.w:427g, m.p.175°C; R_f = 0.6 (20% Ethyl acetate in Hexane); FT-IR (KBr,cm^{-1}): 1655 (C=O), 1594 (C=C Ar), 1537 (CH=CH), 1026 (Ar C-H), 2927 (Alkyl C-H stretching),1516 (NO_2); ^{1}H NMR (400 MHz, $CDCl_3$, ppm), δ: 7.077 (1H, d, J = 16Hz CO-CH=), 7.330 (1H, d, J = 18Hz, Ar-CH=), 1.503 (9H, s, tert-butyl), 2.126 (6H,s,Ar-CH_3), 7.781 (2H,d,C-2",6" Ar-H),8.317(2H,d,C-3",5" Ar-H). Elm. Anal. Calcd.for $C_{21}H_{21}N_3O_7$: C, 59.01%; H, 4.95%; O, 26.20%. Found: C, 59%; H, 4.7%; O, 26%.

R7:Synthesis of (E)-1-(4'-tert-butyl-2',6'-dimethyl-3',5'-dinitrophenyl)-3-(3"- bromophenyl) -2-propen-1-one : Yield: 75%; m.w:461g, m.p.177°C ; R_f = 0.6 (20% Ethyl acetate in Hexane); FT-IR (KBr,cm^{-1}): 1710 (C=O), 1652 (C=C Ar), 1537 (CH=CH), 1026 (Ar C-H), 2926 (Alkyl C-H stretching),1469 (NO_2), 675 (Ar C-Br);); ^{1}H NMR (400 MHz, $CDCl_3$, ppm), δ: 6.972 (1H, d, J = 16Hz CO-CH=), 7.238 (1H, d, J = 16Hz, Ar-CH=), 1.507 (9H, s, tert-butyl), 2.119 (6H,s,Ar-CH_3),7.286–7.745(4H,m,C-2",4'',5",6'', Ar-H), Elm. Anal. Calcd.for $C_{21}H_{21}BrN_2O_5$: C, 54.68%; H, 4.59%; O, 17.32%. Found: C, 54%; H, 4.2%; O, 17%.

R8:Synthesis of (E)-1-(4'-tert-butyl-2',6'-dimethyl-3',5'-dinitrophenyl)-3-(4"- bromophenyl)-2-propen-1-one:Yield: 85%; m.w:461g m.p.177°C; R_f = 0.6 (20% Ethyl acetate in Hexane); FT-IR (KBr,cm^{-1}): 1652

(C=O),1622 (C=C Ar), 1584 (CH=CH), 1011 (Ar C-H), 2926 (Alkyl C-H stretching), 1534 (NO_2), 689 (Ar C-Br); ^{1}H NMR (400 MHz, $CDCl_3$, ppm), δ: 6.968 (1H, d, J = 16Hz CO-CH=), 7.245 (1H, d, J = 16Hz, Ar-CH=), 1.500 (9H, s, tert-butyl), 2.115 (6H,s,Ar-CH_3),7.472(2H,d,C-2",6"Ar-H),7.605(2H,d,C-3",5"Ar-H), Elm.Anal.Calcd.for$C_{21}H_{21}BrN_2O_5$: C, 54.68%; H, 4.59%; O, 17.32%. Found: C, 54%; H, 4.2%; O, 17%.

R9:Synthesis of (E)-1-(4'-tert-butyl-2',6'-dimethyl-3',5'-dinitrophenyl)-3-(3",4"-Methylendioxy phenyl)-2-propen-1-one : Yield: 75%; m.w:426g, m.p.198°C ; R_f = 0.6 (20% Ethyl acetate in Hexane); FT-IR (KBr,cm^{-1}): 1641 (C=O), 1616 (C=C Ar), 1594 (CH=CH), 1032 (Ar C-H), 2922 (Alkyl C-H stretching),1544 (NO_2), 1255 (Ar C-O-C); ^{1}H NMR (400 MHz, $CDCl_3$, ppm), δ: 6.805 (1H, d, J = 16Hz CO-CH=), 7.197 (1H, d, J = 16Hz, Ar-CH=), 1.480 (9H, s, tert-butyl), 2.102 (6H,s,Ar-CH_3), 6.053 (2H,s, -CH_2), 6.837-7.093 (3H, m,Ar-H), Elm. Anal. Calcd.for $C_{22}H_{22}N_2O_7$: C, 61.97%; H, 5.20%; O, 26.26%. Found: C, 61%; H, 5%; O, 26%.

R10:Synthesis of (E)-1-(4'-tert-butyl-2',6'-dimethyl-3',5'-dinitrophenyl)-3-(4"- methoxy phenyl) -2-propen-1-one : Yield: 55%; m.w:412g, m.p. 165°C ; R_f = 0.7 (20% Ethyl acetate in Hexane); FT-IR (KBr,cm^{-1}): 1640 (C=O), 1600 (C=C Ar), 1532 (CH=CH), 1025 (Ar C-H), 2925 (Alkyl C-H stretching),1465 (NO_2), 1207 (Ar C-O-C); ^{1}H NMR (400 MHz, $CDCl_3$, ppm), δ: 6.863 (1H, d, J = 16Hz CO-CH=), 7.244 (1H, d, J = 16Hz, Ar-CH=), 1.503 (9H, s, tert-butyl), 2.126 (6H,s,Ar-CH_3), 3.858(3H,s,OCH3) 7.547 (2H,d,C-2",6" Ar-H),6.949(2H,d,C-3",5" Ar-H), Elm. Anal. Calcd.for $C_{22}H_{24}N_2O_6$: C, 64.07%; H, 5.87%; O, 23.28%. Found: C, 64%; H, 5.5%; O, 23%.

R11:Synthesis of (E)-1-(4'-tert-butyl-2',6'-dimethyl-3',5'-dinitrophenyl)-3-(4"- fluoro phenyl) -2-propen-1-one : Yield: 65%; m.w:400g, m.p.143°C ; R_f = 0.6 (20% Ethyl acetate in Hexane); FT-IR (KBr,cm^{-1}): 1708 (C=O), 1645 (C=C Ar), 1597 (CH=CH), 1026 (Ar C-H), 2925 (Alkyl C-H stretching),1537 (NO_2), 1350 (Ar C-F); ^{1}H NMR (400 MHz, $CDCl_3$, ppm), δ: 7.077 (1H, d, J = 16Hz CO-CH=),7.330 (1H, d, J = 16Hz, Ar-CH=),1.504 (9H, s, tert-butyl), 2.120 (6H,s,Ar-CH_3), 7.781(2H,d,C-2",6"Ar-H), 8.317 (2H,d,C-3",5"Ar-H), Elm.Anal.Calcd.for$C_{21}H_{21}FN_2O_5$: C, 62.99%; H, 5.29%; O, 19.98%. Found: C, 62%; H, 5%; O, 19%.

R12:Synthesis of (E)-1-(4'-tert-butyl-2',6'-dimethyl-3',5'-dinitrophenyl)-3-(4"- hydroxy phenyl) -2-propen-1-one : Yield: 75%; m.w:398g, m.p.177°C ; R_f = 0.6 (20% Ethyl acetate in Hexane); FT-IR (KBr,cm^{-1}): 1687 (C=O), 1655 (C=C Ar), 1627 (CH=CH), 1013 (Ar C-H), 2924 (Alkyl C-H stretching),1510 (NO_2), 3451 (Ar OH); ^{1}H NMR (400 MHz, $CDCl_3$, ppm), δ: 6.953 (1H, d, J = 16Hz CO-CH=), 7.261 (1H, d, J = 16Hz, Ar-CH=), 1.504 (9H, s, tert-butyl), 2.120 (6H,s,Ar-CH_3), 5.255(1H,s, Ar-OH), 7.549 (2H,d,C-2",6" Ar-H),7.425(2H,d,C-3",5" Ar-H), Elm. Anal. Calcd.for $C_{21}H_{22}N_2O_6$: C, 63.31%; H, 5.57%; O, 24.10%. Found: C, 63%; H, 5.2%; O, 24%.

R13:Synthesis of (E)-1-(4'-tert-butyl-2',6'-dimethyl-3',5'-dinitrophenyl)-3-(3",4"- dihydroxy phenyl) -2-propen-1-one : Yield: 75%; m.w:414g, m.p.167°C; R_f = 0.6 (20% Ethyl acetate in Hexane); FT-IR (KBr,cm^{-1}): 1711 (C=O), 1651 (C=C Ar), 1618 (CH=CH), 1030 (Ar C-H), 2926 (Alkyl C-H stretching),1510 (NO_2), 3437 (Ar OH); ^{1}H NMR (400 MHz, $CDCl_3$, ppm), δ: 7.077 (1H, d, J = 16Hz CO-CH=), 7.330 (1H, d, J = 18Hz, Ar-CH=), 1.503 (9H, s, tert-butyl), 2.126 (6H,s, Ar-CH_3), 5.036(2H,s,Ar-OH), 7.371–8.317 (3H, m, C- 2'', 5", 6'', Ar-H), Elm. Anal. Calcd.for $C_{21}H_{22}N_2O_7$: C, 60.86%; H, 5.35%; O, 24.10%. Found: C, 60%; H, 5%; O, 24%.

R14:Synthesis of (E)-1-(4'-tert-butyl-2',6'-dimethyl-3',5'-dinitrophenyl)-3-(3"-ethoxy-4"- hydroxylphenyl) -2-propen-1-one :Yield: 55%; m.w:442g, m.p.148°C; R_f = 0.6 (20% Ethyl acetate in Hexane); FT-IR (KBr,cm^{-1}): 1651 (C=O), 1619 (C=C Ar), 1579 (CH=CH), 1030 (Ar C-H), 2927 (Alkyl C-H stretching),1503 (NO_2), 3445 (Ar OH), 1242 (Ar C-O-C);); ^{1}H NMR (400 MHz, $CDCl_3$, ppm), δ: 7.077 (1H, d, J = 16Hz CO-CH=), 7.330 (1H, d, J = 18Hz, Ar-CH=), 1.480 (9H, s, tert-butyl), 2.102 (6H,s, Ar-CH_3), 5.280(1H,s,Ar-OH), 3.480(5H,s, -OC_2H_5) 7.371–8.317 (3H, m, C- 2'',5",6'', Ar-H), Elm. Anal. Calcd.for $C_{21}H_{20}Cl_2N_2O_5$: C, 62.43%; H, 5.92%; O, 25.31%. Found: C, 62%; H, 5.2%; O, 25%.

R15: Synthesis of (E)-1-(4'-tert-butyl-2',6'-dimethyl-3',5'-dinitrophenyl)-3-(1H-pyrrol-2-yl) -2-propen-1-one : Yield: 75%; m.w:371g, m.p.165°C; R_f =0.6 (20% Ethyl acetate in Hexane); FT-IR (KBr,cm^{-1}): 1713 (C=O), 1646 (C=C Ar), 1611 (CH=CH), 1129 (Ar C-H), 2924 (Alkyl C-H stretching),1532 (NO_2),3428 (-NH),1460 (C-N); ^{1}H NMR (400 MHz, $CDCl_3$, ppm), δ: 7.077 (1H, d, J = 16Hz CO-CH=), 7.330 (1H, d, J =

18Hz, Ar-CH=), 1.480 (9H, s, tert-butyl), 2.102 (6H,s, Ar-CH_3), 5.280(1H,s,Ar-OH), 3.480(5H,s, -OC_2H_5) 7.371–8.317 (3H, m, C- 3′′, 4”, 5′′, Ar-H), Elm. Anal. Calcd.for $C_{19}H_{21}N_3O_5$: C, 61.45%; H, 5.70%; O, 21.54%. Found: C, 61%; H, 5.2%; O, 21%.

R16:Synthesis of (E)-1-(4’-tert-butyl-2’,6’-dimethyl-3’,5’-dinitrophenyl)-3-(thiophen-2”-yl) -2-propen-1-one : Yield: 55%; m.w:388g, m.p.195°C ; R_f = 0.6 (20% Ethyl acetate in Hexane); FT-IR (KBr,cm^{-1}): 1704 (C=O), 1605 (C=C Ar), 1640 (CH=CH), 1036 (Ar C-H), 2924 (Alkyl C-H stretching),1531 (NO_2),834 (C-S); ^{1}H NMR (400 MHz, $CDCl_3$, ppm), δ: 6.764 (1H, d, J = 16Hz CO-CH=), 7.574 (1H, d, J = 16Hz, Ar-CH=), 1.504 (9H, s, tert-butyl), 2.130 (6H,s,Ar-CH_3), 7.138–7.428 (3H, m, C- 3′′, 4”, 5′′, Ar-H), Elm. Anal. Calcd.for $C_{19}H_{20}N_2O_5S$: C, 58.75%; H, 5.19%; O, 20.18%. Found: C, 58%; H, 5%; O, 20%.

R17:Synthesis of (E)-1-(4’-tert-butyl-2’,6’-dimethyl-3’,5’-dinitrophenyl)-3-(4”- methyl phenyl) -2-propen-1-one : Yield: 75%; m.w:396g m.p.160°C ; R_f = 0.6 (20% Ethyl acetate in Hexane); FT-IR (KBr,cm^{-1}): 1710 (C=O), 1646 (C=C Ar), 1537 (CH=CH), 1027 (Ar C-H), 2924 (Alkyl C-H stretching),1463 (NO_2); ^{1}H NMR (400 MHz, $CDCl_3$, ppm), δ: 6.863 (1H, d, J = 16Hz CO-CH=), 7.244 (1H, d, J = 16Hz, Ar-CH=), 1.503 (9H, s, tert-butyl), 2.126 (6H,s,Ar-CH_3), 3.858(3H,s,CH3),7.547 (2H,d,C-2”,6” Ar-H),6.949(2H,d,C-3”,5” Ar-H), Elm. Anal. Calcd.for $C_{21}H_{24}N_2O_5$: C, 66.65%; H, 6.10%; O, 20.18%. Found: C, 66%; H, 6%; O, 20%.

R18:Synthesis of (E)-1-(4’-tert-butyl-2’,6’-dimethyl-3’,5’-dinitrophenyl)-3-(2”,4”- difluoro phenyl) -2-propen-1-one: Yield: 65%; m.w:418g, m.p.136°C; R_f = 0.6 (20% Ethyl acetate in Hexane); FT-IR (KBr,cm^{-1}): 1651 (C=O), 1622 (C=C Ar), 1583 (CH=CH), 1048 (Ar C-H), 2925 (Alkyl C-H stretching),1534 (NO_2), 1356 (Ar C-F); ^{1}H NMR (400 MHz, $CDCl_3$, ppm), δ: 6.909 (1H, d, J = 16Hz CO-CH=), 7.704 (1H, d, J = 16Hz, Ar-CH=), 1.497 (9H, s, tert-butyl), 2.137 (6H,s, Ar-CH_3),7.285–7.625 (3H, m, C- 3′′, 5′′, 6′′, Ar-H), Elm. Anal. Calcd.for $C_{21}H_{20}F_2N_2O_5$: C, 60.28%; H, 4.82%; O, 19.12%. Found: C, 60%; H, 4.2%; O, 19%.

R19:Synthesis of (E)-1-(4’-tert-butyl-2’,6’-dimethyl-3’,5’-dinitrophenyl)-3-(3”,4”- dimethoxy phenyl)-2-propen-1-one : Yield: 55%; m.w:442g m.p. 148°C; Rf = 0.6 (20% Ethyl acetate in Hexane); FT-IR (KBr,cm−1): 1651 (C=O), 1619 (C=C Ar), 1579 (CH=CH), 1030 (Ar C-H), 2927 (Alkyl C-H stretching),1503 (NO2),1242 (Ar C-O-C)’ 1H NMR (400 MHz, CDCl3, ppm), δ: 7.077 (1H, d, J = 16Hz CO-CH=), 7.330 (1H, d, J = 18Hz, Ar-CH=), 1.503 (9H, s, tert-butyl), 2.126 (6H,s, Ar-CH3), 3.940 (6H,s, Ar-OCH3), 7.371–8.317 (3H, m, C- 2′′, 5”, 6′′, Ar-H), Elm. Anal. Calcd.for C23H26N2O7: C, 62.423%; H, 5.92%; O, 25.31%. Found: C, 62%; H, 5.3%; O, 25%.

R20: Synthesis of (E)-1-(4’-tert-butyl-2’, 6’-dimethyl-3’, 5’-dinitro phenyl)-3-(pyridin-4”-yl) -2-propen-1-one : Yield: 75%; m.w:383g, m.p.150°C ; R_f = 0.6 (20% Ethyl acetate in Hexane); FT-IR (KBr,cm^{-1}): 1655 (C=O), 1594 (C=C Ar), 1537 (CH=CH), 1025 (Ar C-H), 2927 (Alkyl C-H stretching),1515 (NO_2), 1467 (C=N); ^{1}H NMR (400 MHz, $CDCl_3$, ppm), δ: 6.953 (1H, d, J = 16Hz CO-CH=), 7.261 (1H, d, J = 16Hz, Ar-CH=), 1.504 (9H, s, tert-butyl), 2.120 (6H,s,Ar-CH_3), 7.447 (2H, d, C-2”,6” Ar-H),7.549(2H, d, C-3”,5” Ar-H), Elm. Anal. Calcd.for $C_{20}H_{21}N_3O_5$: C, 62.66%; H, 5.52%; O, 20.87%. Found: C, 62%; H, 5%; O, 20%.

2.3 Antimicrobial Evaluation

The antibacterial activity was tested using serial dilution to ascertain each compound's minimum inhibitory concentration (MIC) [46]. The organisms listed below were employed.

Gram-positive bacteria	*Staphylococcus aureus* (NCIM-2079), *Bacillus subtilis* (NCIM 2063)
Gram-negative bacteria	*Escherichia coli* (NCIM-2068), *Proteus vulgaris* (NCIM-2027)
Fungi	*Aspergillus niger* (ATCC-6275), *Candida tropicalis* (ATCC-1369)

The MIC—the lowest dose of the compound that inhibited each strain's growth following an overnight incubation period—was used to evaluate the antibacterial activity of the chalcones (R1 to R20). MIC levels can be found using several common test methods. Agar and tube dilution are the two most widely used techniques to verify if pathogens are resistant to an antimicrobial agent and to track the effectiveness of novel antimicrobial agents. The serial tube method was used in the current study to estimate the MIC. The test organisms were inoculated into broth medium tubes

containing graded chemical dosages. Growth occurred inside the tubes where the chemical concentration was below the inhibitory level, and the culture turned turbid after the appropriate incubation. The tubes retained clear, and no growth was observed above the inhibitory threshold.

1. Preparation of the sample solution: Each test chemical was taken separately in vials containing 2.048 mg. Two milliliters of methanol were then added. Consequently, a solution containing 1.024 mg/mL was produced.

2. Preparation of the inoculums: The sterile nutritional broth medium was used to dilute the test bacteria, cultivated at 37^0C in nutrient agar medium until the suspension contained roughly 10^7 cells/mL. As the inoculum, this suspension was employed.

3. Procedure:

Nine of the eleven test tubes were labeled 1, 2, 3, 5, 6, 7, 8, and 9, while the remaining two were designated as TM (medium) and TMI (medium+inoculum). Each of the 11 test tubes received 1 milliliter of the nutrient broth medium. After being cotton-plugged, these test tubes were autoclave-sterilized at a pressure of 15 pounds per square inch. Following cooling, 1 milliliter of the sample solution was added to the first test tube, thoroughly mixed, and then moved to the second test tube. After thoroughly mixing the contents of the second test tube, 1 mL was once more moved to the third test tube. The same serial dilution procedure was followed up to the ninth test tube. Each of the nine test tubes received 10 µL of the appropriately diluted inoculum, which was thoroughly mixed. A total of 10 µL of the inoculum was put into the test tube TMI to see how the organism grew in the media. The sterility of the medium was verified using a controlled test tube TM that contained only the medium. All test tubes were then incubated for eighteen hours at 37°C.

A control experiment was performed with a medium, methanol, and an inoculum without the test substance to confirm that methanol did not interfere with the dilutions. The test tube where the initial growth of the organism was observed was noted. The concentration in the tube immediately preceding the one where growth was first detected was identified as the MIC. This procedure determined the MIC values and standard for the tested compounds. A similar method was employed to assess antifungal activity, except for using the potato-dextrose-agar medium.

2.4. Molecular docking

2.4.1. Protein and ligand preparation

The RCSB protein data bank provided the previously published 3D crystal structure of glucosamine-6P synthase with PDB: 4AMV and $2.05A^0$ resolution (available at https://www.rcsb.org/). Furthermore, water molecules and previously bound ligand groups were eliminated to clean and prepare the downloaded protein structure. Polar hydrogen atoms were also added to the protein structure to protonate it. All the protein preparation tasks were done using BIOVIA Discovery Studio [47]. The 2D structures of the prepared chalcones (R1 to R20) as ligands were drawn using the ChemSketch chemical drawing tool; these structures were saved in MOL format and uploaded to the AutoDock Vina module in the PyRx 0.8 software package for docking studies.

2.4.2. Validation of protein structure

The validation of protein structures is particularly important *in silico* studies as these rely heavily on the accuracy and quality of computational models for a variety of applications in drug discovery. For protein-ligand docking, accurate protein structures are critical for docking studies, as errors can lead to incorrect predictions of binding sites, binding affinities, or ligand orientations. In this study, the PROCHECK, ERRAT, PROVE, and Verify 3D tools from the SAVES server (available at https://saves.mbi.ucla.edu/) and the online ProSA-web server (available at https://prosa.services.came.sbg.ac.at/prosa.php) were used for validating and evaluating the quality of the produced protein structure (PDB: 4AMV) to determine the overall QMEAN score [48-52].

2.4.3. Active site prediction

Predicting active sites helps locate regions of proteins that can bind to small molecules, guiding the design of inhibitors or activators. Understanding active sites' geometry and chemical properties enables the rational design of compounds that specifically interact with the target protein. Predicted active sites are used to dock

virtual libraries of compounds, accelerating the identification of lead molecules. In this study, the validated protein structure (PDB: 4AMV) was analyzed for binding pocket compatibility using the active site prediction server CASTp (available at http://sts.bioe.uic.edu/castp/index.html?4jii) [53] and BIOVIA Discovery Studio. The CASTp server identifies multiple binding pockets with distinct surface areas, volume dimensions, and residue counts. For docking analysis, this study selected the binding pocket with the largest surface area (1320.615Å 2) and volume (753.247Å 3).

2.4.4. Molecular docking studies

Using the Auto Dock Vina package of PyRx 0.8 (available at https://pyrx.sourceforge.io/), [54-57] molecular docking was carried out for 20 chalcones (R1 to R20) with the protein (4AMV). PyRx 0.8 loaded the target protein's PDB file format, which was subsequently transformed into a macromolecule in the PDBQT file format. The PyRx Open Babel plugin was used to apply energy minimization (EM) to the ligand structure and convert it to the PDBQT format. A grid box was chosen to cover the binding site residues using dimensions obtained from CASTp (Computed Atlas of Surface Topology of Protein) after the ligand structures and the targeted protein were chosen in Auto Dock Vina, using the Vina workspace, X: 27.92, Y: 35.65, and Z: 32.54 with center X: 7.193, Y: 3.008, and Z: 92.020. By default, the exhaustiveness was set to 8 for every ligand, and the optimal position with the greatest negative binding affinity and zero RMSD was chosen. Additionally, using BIOVIA Discovery Studio, the interaction between the docked protein and ligand was visualized, and stored conformations were examined.

3. Results and Discussion

3.1. Chemistry

The data provided for the synthesized chalcones (R1to R20) includes their IR and ^{1}H NMR spectral characteristics and elemental analysis, revealing critical insights into their structural and functional properties. In the IR spectra, the strong absorption bands between 1600–1710 cm^{-1} and 1500-1600 cm^{-1} correspond to C=O stretching vibrations and C=C stretching vibrations, confirming the presence of α, β-unsaturated ketone functional group typical of chalcones [58-59]. Additional bands in the regions 1000-1050, 3000–3100 cm^{-1}, and 2900–3000 cm^{-1} indicate aromatic C–H and aliphatic C–H stretching, respectively. The peaks at 1550–1650 cm^{-1} are associated with C=C aromatic stretching; compounds containing nitro ($-NO_2$) groups exhibit characteristic absorption bands near 1500 cm^{-1} and 1300 cm^{-1}, while halogen substituents contribute to low-intensity bands around 850 cm^{-1} and 1350 cm^{-1}. In the ^{1}H NMR spectra, signals in the δ 6.5–8.5 ppm range are attributed to aromatic protons, confirming the conjugated aromatic rings in chalcone scaffolds. The doublets observed at δ 6.5–8.5 ppm with coupling constant (*J*) of 16 Hz are diagnostic for trans-olefinic protons, consistent with the α, β-unsaturated system [60-62]. Aliphatic protons from methyl groups appear at δ 1.45 – 4.0 ppm, while substituents such as hydroxyl (-OH) or methoxy ($-OCH_3$) are indicated by singlets in the δ 3.5–5.5 ppm range. Nitro and halogen groups influence the chemical shifts and splitting patterns, supporting the substitution positions on the aromatic rings.

The elemental analysis shows good agreement between the calculated and experimental carbon, hydrogen, and oxygen percentages, validating the proposed molecular compositions. Variations in functional groups (e.g., halogen, nitro, methoxy) across R1 to R20 significantly influence the spectroscopic patterns, emphasizing their role in modulating electronic and steric properties. Overall, the IR and NMR results, alongside elemental analysis, provide comprehensive structural confirmation of the chalcones, highlighting their conjugated systems and diverse functional groups. These properties are fundamental for their reactivity and potential applications in medicinal chemistry.

3.2 Antimicrobial Evaluation

3.2.1. Antibacterial Activity:

Table 2 shows the MIC values for the antibacterial activity of chalcones (R1 to R20) against gram-positive and gram-negative organisms. The findings make it clear that all the synthesized chalcones exhibited antibacterial activity against the tested species but with varying minimum inhibitory concentrations (MICs) that were not equivalent to the standard (ciprofloxacin).

Table 2. Antibacterial activity of chalcones (R1 to R20). (MIC is expressed in µg/mL)

Compound code	R	Gram +ve organisms		Gram-ve organisms	
		Bacillus subtilis	***Staphilococcus aureus***	***E. coli***	***Proteus vulgaris***
R1	2",4"-dichlorphenyl	32	32	32	32
R2	4"-chlorophenyl	64	64	32	64
R3	3",4",5"-trimethoxyphenyl	64	64	64	64
R4	4"-dimethylaminophenyl	128	64	128	128
R5	3"-nitrophenyl	32	32	32	32
R6	4"-nitrophenyl	32	32	32	32
R7	3"-bromophenyl	128	64	128	128
R8	4"-bromophenyl	128	64	256	128
R9	3",4"-methylendioxyphenyl	64	64	64	64
R10	4"-methoxyphenyl	128	256	256	128
R11	4"-fluorophenyl	64	64	64	128
R12	4"-hydroxyphenyl	256	128	256	256
R13	3",4"-dihydroxyphenyl	256	256	128	256
R14	3"-ethoxy-4"- hydroxyphenyl	256	128	256	128
R15	2"-pyrrolyl	128	128	128	64
R16	2"-thienyl	128	128	128	64
R17	4"-methylphenyl	128	256	128	128
R18	2",4"-difluorophenyl	32	32	32	32
R19	3",4"-dimethoxyphenyl	128	64	64	128
R20	4"-pyridinyl	128	128	128	64
Ciprofloxacin (STD)		< 2	< 2	< 2	< 2

With a MIC value of 32 µg/mL in each instance, R1 (chlorophenyl), R5 (3-nitro phenyl), R6 (4-nitro phenyl), and R18 (difluorophenyl) were determined to be the most effective drugs against gram-positive and gram-negative organisms among those examined. The chalcones R2 (chlorophenyl), R3 (trimethoxyphenyl), R9 (methylenedioxyphenyl), and R11 (fluorophenyl) showed moderately effective against both gram-positive and gram-negative microorganisms having a MIC value of 64 µg/mL in each case. However, most of the synthesized chalcones exhibited higher MIC values, ranging from 128 to 256 µg/mL, reflecting reduced antibacterial potency. The structure-activity relationship (SAR) analysis highlights the critical role of electron-withdrawing groups in enhancing antibacterial activity [63-65]. Compounds such as R1 and R18, with dichloro and difluoro substitutions, respectively, demonstrated a cumulative effect on activity when multiple electron-withdrawing groups were present on the phenyl ring. Similarly, nitro-substituted compounds like R5 and R6 also exhibited enhanced antibacterial activity, underscoring the importance of these groups. Interestingly, compounds with electron-releasing substituents, such as R3 (trimethoxyphenyl) and R9 (methylenedioxyphenyl), also displayed moderate activity, suggesting that such groups can contribute positively to antibacterial potency under certain conditions. These findings imply that electron-withdrawing and electron-releasing groups can influence activity through different mechanisms. Future studies should focus on synthesizing chalcones with varying numbers and positions of electron-withdrawing and electron-releasing substituents on aromatic or heteroaromatic rings to further elucidate the impact of electronic effects on antimicrobial activity. This approach may provide deeper insights into the influence of electronic effects on antibacterial activity and aid in designing more potent chalcone derivatives.

3.2.2. Antifungal Activity:

Table 3 shows the MIC values for the antifungal activity of chalcones (R1 to R20) against the examined organisms. It is evident from the results that all of the synthesized chalcones exhibited antifungal efficacy against the tested organisms but with varying minimum inhibitory concentrations (MICs) that were not equivalent to the standard (fluconazole).

Table 3. Antifungal activity of chalcones (R1 to R20). (MIC is expressed in µg/mL)

Compound code	R	*Aspergillus niger*	*Candida tropicalis*
R1	2",4"-dichlorphenyl	16	16
R2	4"-chlorophenyl	32	32
R3	3",4",5"-trimethoxyphenyl	16	16
R4	4"-dimethylaminophenyl	128	128
R5	3"-nitrophenyl	128	128
R6	4"-nitrophenyl	128	128
R7	3"-bromophenyl	128	128
R8	4"-bromophenyl	64	64
R9	3",4"-methylendioxyphenyl	64	64
R10	4"-methoxyphenyl	128	128
R11	4"-fluorophenyl	32	32
R12	4"-hydroxyphenyl	32	32
R13	3",4"-dihydroxyphenyl	256	256
R14	3"-ethoxy-4"- hydroxyphenyl	256	256
R15	2"-pyrrolyl	128	128
R16	2"-thienyl	128	128
R17	4"-methylphenyl	128	256
R18	2",4"-difluorophenyl	16	16
R19	3",4"-dimethoxyphenyl	128	128
R20	4"-pyridinyl	128	64
Fluconazole (STD)		< 2	< 2

With a MIC value of 16µg/mL against A. niger and C. tropicalis, compounds R1, R3, and B18 were shown to be the most effective among those evaluated for antifungal activity. The dual activity of R1 and R18 underscores the importance of their dichlorophenyl and difluorophenyl moieties in contributing favorably to antibacterial and antifungal activities. With MIC values of 32 µg/mL, the chalcones R2, R11, and R12, each of which included a distinct electron-withdrawing or electron-releasing substituent, demonstrated antifungal activity. The other drugs were likewise found to be moderately potent, with MIC values ranging from 64 to 256 µg/mL. According to the Structure-Activity Relationship (SAR), antifungal activity is greatly increased when halogens such as fluorine and chlorine are present at various locations on the phenyl ring [66].

Furthermore, as indicated by R3, electron-releasing groups, such as three methoxy groups at positions 3, 4, and 5 of the phenyl ring, also seem to increase inhibitory activity [67]. These findings highlight the crucial role of both electron-withdrawing and electron-releasing substituents in modulating antifungal potency. Future studies should focus on synthesizing chalcones with multiple substituents on the aromatic ring to further explore and enhance antifungal activity, strategically incorporating electron-withdrawing and electron-releasing groups at various positions. This approach holds promise for developing more potent antifungal chalcone derivatives.

3.3. Validation of Protein structure

Various online tools were utilized to assess the quality of the generated protein structure for PDB: 4AMV. The Ramachandran plot, created using the PROCHECK server, revealed that 92.7% of the residues are located in favored regions, as illustrated in **Figure 1a**. This indicates a well-refined protein model. ERRAT analysis further supported this by reporting an overall quality

factor of 97.830% for the structure (**Figure 1b**). The Verify 3D analysis also showed that 83.39% of the amino acid residues achieved an average score greater than 0.1, confirming a consistent match between the atomic 3D model and the 1D amino acid sequence (**Figure 1c**). The ProSA-web server provided z-scores of −7.55 for all chains in the structure, which are represented as black dots in **Figure 1d**. These scores, calculated based on chain lengths determined by X-ray crystallography (light blue) or NMR spectroscopy (dark blue), further confirm the structural accuracy of the model. Moreover, the ProSA-web energy plot (**Figure 1e**) illustrates local model quality, with a thick green line representing the average energy for each 40-residue fragment and a thin green line indicating the average energy for a window size of 10 residues [48-52]. These analyses collectively validate the suitability of the PDB: 4AMV structure for further molecular docking studies. The high percentage of residues in favored regions, the excellent quality factor from ERRAT, and the alignment of the atomic model with the amino acid sequence confirm that the protein structure is robust and reliable. These findings enhance confidence in its application for subsequent computational or experimental research, particularly in exploring protein-ligand interactions.

3.4. Active Site Prediction

Binding pocket analysis performed using CASTp and BIOVIA Discovery Studio revealed a series of key amino acid residues within the binding pocket of the protein structure PDB: 4AMV. These critical residues include CYS 1, ARG 26, HIS 71, ARG 73, THR 76, GLU 79, ASN 84, GLY 175, SER 176, PRO 177, SER 191, ASP 192, GLN 193, CYS 300, GLY 301, THR 302, GLN 348, SER 349, GLU 351, THR 352, ALA 353, ASN 375, SER 379, VAL 376, SER 401, LEU 484, LEU 601, LYS 603, SER 604, and VAL 605. These residues play a significant role in the binding interactions within the pocket and are represented by yellow spheres in **Figure 2**. Identifying and visualizing these key residues are crucial for understanding the potential binding sites for ligands and developing effective therapeutic strategies. These amino acids contribute to the structural and functional integrity of the binding pocket, suggesting their involvement in protein-ligand interactions that could be leveraged in drug design.

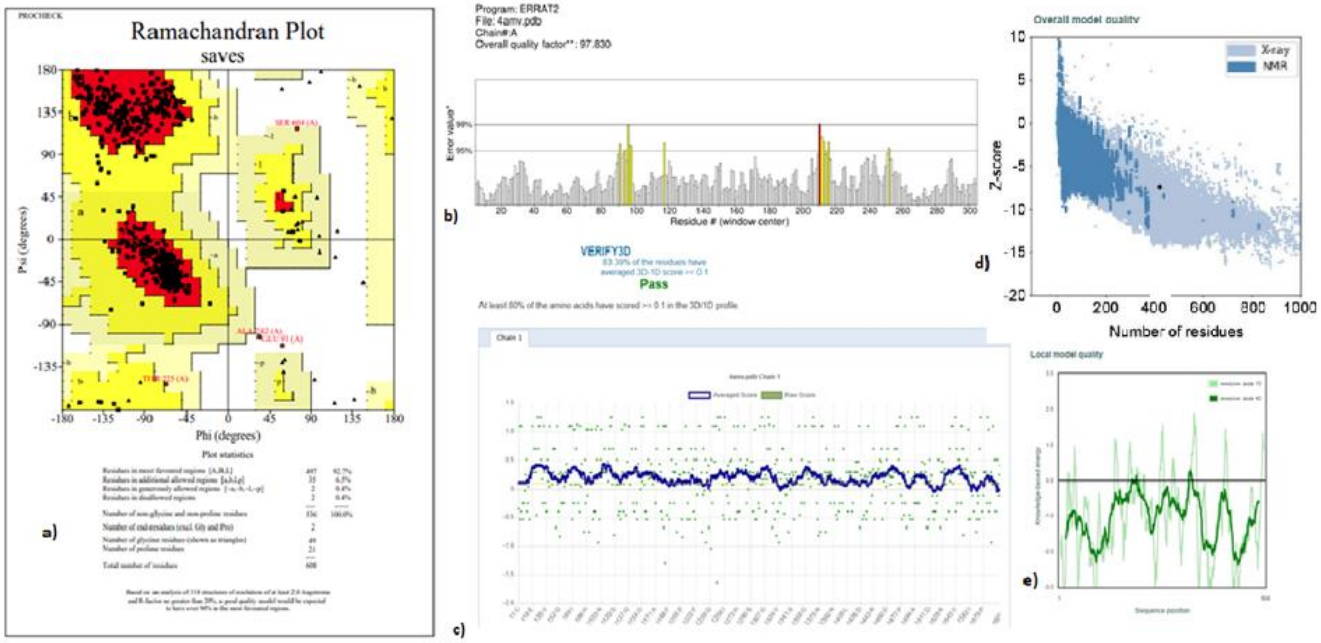

Figure 1. Validation and quality assessment of the prepared protein structure (PDB:4AMV) using a) the PROCHEK Ramachandran plot, b) ERRAT, and c) a 3D plot that confirms the amino acids in the preferred regions. d) The model's overall quality, and e) The local model quality as seen through ProSA-web.

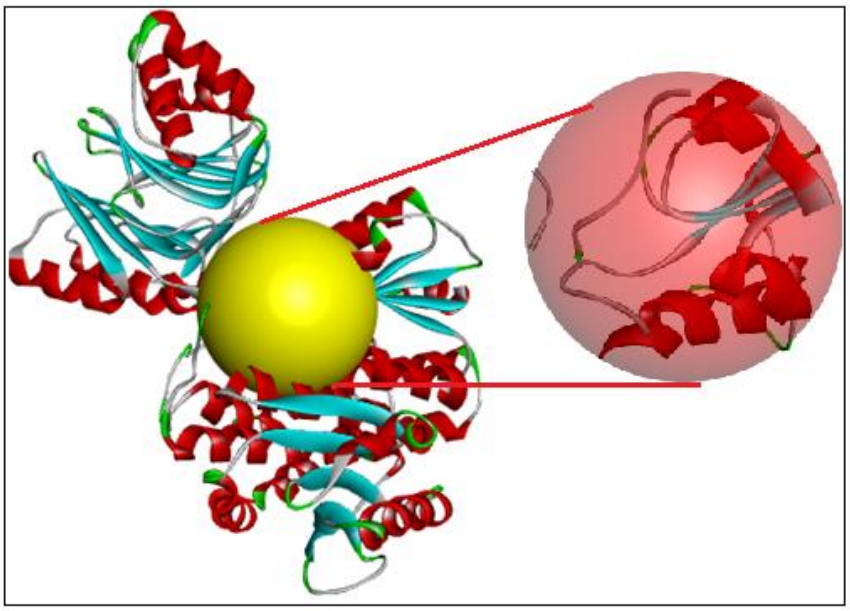

Figure 2. The predicted active site of glucosamine-6P synthase (PDB ID: 4AMV) using BIOVIA Discovery Studio and the CASTp server. The yellow sphere highlighted in PDB ID 4AMV indicates the binding pocket that has been found.

3.5. Molecular Docking Studies

A docking study was conducted using twenty chalcones (R1 to R20) as ligands and ciprofloxacin (STD) with the protein PDB: 4AMV, yielding binding affinities ranging from -7.2 to -8.4 kcal/mol, as summarized in **Table 4**. The four ligands with the highest negative binding affinities (R6, R1, R5, and R9) were selected for further docking analysis.

Table 5 provides detailed information on the binding affinities, number of hydrogen bonds, and residual interactions of these top four ranked ligands along with ciprofloxacin (STD).

Table 4. Binding affinity of ciprofloxacin and chalcones (R1 to R20).

S.No	Compound code	Binding affinity (K.cal/mol)	S.No	Compound code	Binding affinity (K.cal/mol)
1	R1	-8.2	11	R11	-7.5
2	R2	-7.5	12	R12	-7.4
3	R3	-7.5	13	R13	-7.4
4	R4	-7.5	14	R14	-7.7
5	R5	-8.2	15	R15	-7.2
6	R6	-8.4	16	R16	-7.2
7	R7	-7.4	17	R17	-7.6
8	R8	-7.6	18	R18	-7.7
9	R9	-8	19	R19	-7.5
10	R10	-7.4	20	R20	-7.3
Ciprofloxacin (STD)			-8.3		

Table 5. The binding affinity of ciprofloxacin (STD) and top four ranked chalcones against Glucosamine-6P synthase (PDB ID: 4AMV) along with the interacting residues and type of interaction.

S.No	Compound code	Binding affinity (K.cal/mol)	No of hydrogen bonds	Interacting residues	Distance (Å)	Type of interaction
1	Ciprofloxacin (STD)	-8.3	4	GLN 348 LYS 603 SER 604 SER 604 SER 349 CYS 300 VAL 605	1.99 1.78 2.65 2.73 3.48 4.54 4.28	Conventional HB Conventional HB Conventional HB Conventional HB Carbon HB Pi-Alkyl Pi-Alkyl
2	R6	-8.4	3	CYS 1 GLN 193 GLN 348 PRO 177 VAL 376 ASP 192 ARG 26	2.21 2.59 2.34 3.72 4.18 2.99 2.97	Conventional HB Conventional HB Conventional HB Pi-Alkyl Pi-Sigma Pi-Cation Pi-Anion
3	R1	-8.2	2	GLN 193 GLN 348 PRO 177 VAL 376 ASP 192 ARG 26	2.43 2.50 3.66 4.50 2.98 3.14	Conventional HB Conventional HB Pi-Alkyl Pi-Sigma Pi-Cation Pi-Anion
4	R5	-8.2	3	SER 401 VAL 605 THR 352 LEU 601 GLY 301 THR 302 CYS 300	2.33 2.03 2.44 4.52 3.01 2.99 4.66	Conventional HB Conventional HB Conventional HB Pi-Sigma Carbon HB Carbon HB Amide Pi Stacked
5	R9	-8	3	SER 401 VAL 605 THR 352 THR 302 LEU 484	2.50 2.00 2.31 3.15 5.32	Conventional HB Conventional HB Conventional HB Carbon HB Pi-Alkyl

Figure 3 illustrates the superimposed structures of the top four ranked ligands and ciprofloxacin within the active site of PDB: 4AMV, as predicted by the CASTp server and BIOVIA Discovery Studio. Additionally, **Figures 4** and **5** depict the docking poses of ciprofloxacin and the top four ranked ligands forming complexes with PDB: 4AMV.

The docking results of the ligands R6, R1, R5, and R9 with the protein PDB: 4AMV demonstrate significant binding affinities and specific particular interactions at the protein's active site. Ciprofloxacin, used as the reference standard, exhibited a binding affinity of -8.3 kcal/mol, forming four hydrogen bonds with residues such as GLN348, LYS603, and SER604 (2), in addition to hydrophobic interactions like Pi-Alkyl. Among the four ligands, R6 displayed the highest binding affinity (-8.4 kcal/mol), forming three hydrogen bonds with residues like CYS1, GLN193, and GLN348. It also interacted through hydrophobic interactions such as Pi-Alkyl and Pi-Cation. This suggests that R6 effectively stabilizes within the binding pocket, making it a strong candidate for further consideration. Ligands R1 and R5 showed identical binding affinities of -8.2 kcal/mol. R1 formed two hydrogen bonds, interacting primarily with GLN193 and GLN348, complemented by Pi-Sigma and Pi-Anion interactions. R5, on the other hand, formed three hydrogen bonds, engaging residues such as THR 352, SER401, and VAL605, alongside Pi-Sigma and Carbon Hydrogen interactions.

The additional hydrogen bond in R5 may contribute to its comparable binding affinity with R1 despite differing interaction profiles.R9 demonstrated a binding affinity of -8.0 kcal/mol, forming three hydrogen bonds with residues such as THR352, SER401, and VAL605. Additionally, it showed strong hydrophobic interactions, including Pi-Alkyl, which may enhance its binding stability within the active site. Overall, the top ligands (R6, R1, R5, and R9) exhibit competitive binding affinities and interactions relative to ciprofloxacin. The differences in hydrogen bonding and hydrophobic interactions highlight the importance of specific molecular features in achieving optimal binding. These results suggest that R6, in particular, warrants further investigation due to its superior binding affinity and robust interaction profile.

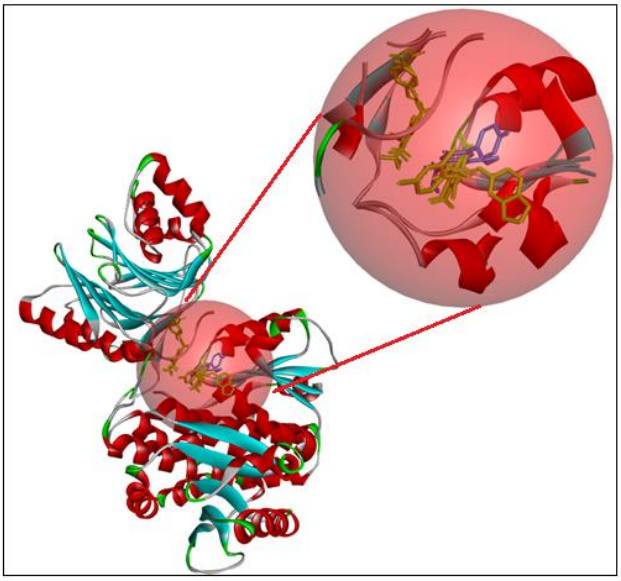

Figure 3. The red sphere that is highlighted indicates the binding pocket that has been found in glucosamine-6P synthase (PDB ID: 4AMV). Superimpose of the top four ranked chalcones (R6, R1, R5, and R9) represented in green color stick model and ciprofloxacin (STD) represented in blue color stick model.

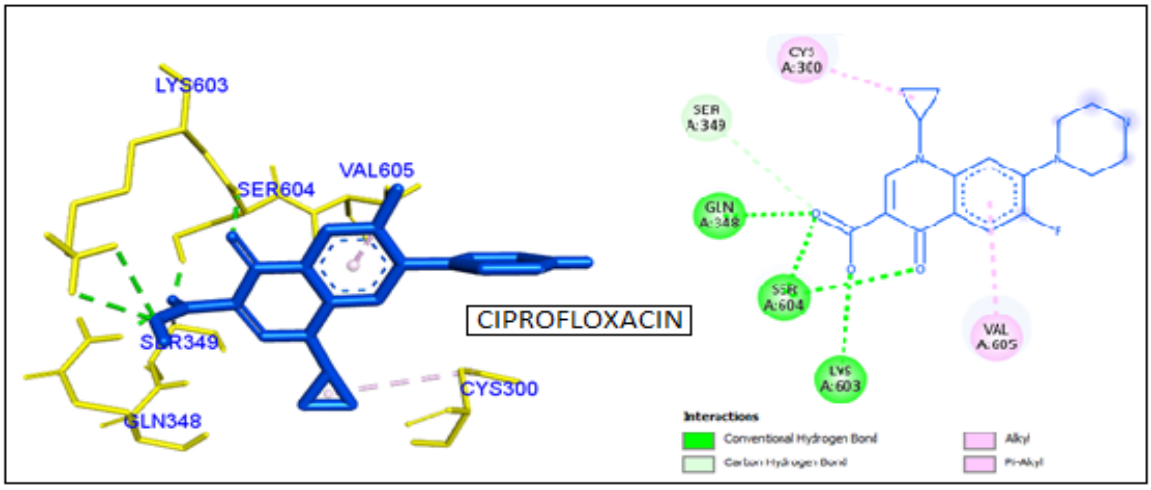

Figure 4. Binding interactions of Ciprofloxacin (STD) at the active site of Glucosamine-6P synthase (PDB ID: 4AMV) along with their 2D interactions. The interacting residues of the protein are represented in the yellow color stick model, and Ciprofloxacin (STD) is represented in the blue color stick model. The conventional hydrogen bonds are represented in the green color, and non-covalent interactions are represented in the pink color.

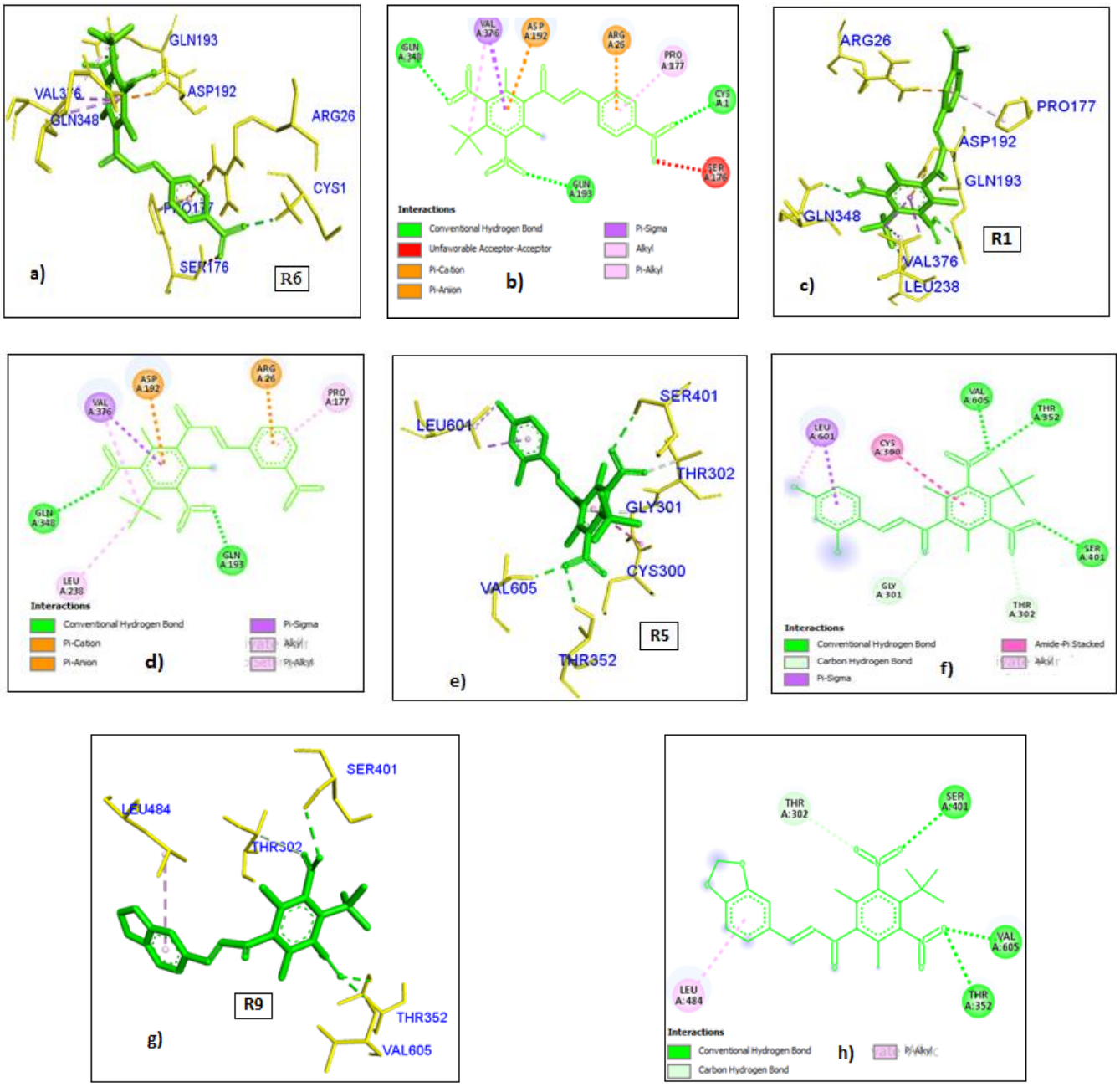

Figure 5 (a-h). Binding interactions of the top four ranked chalcones (R6, R1, R5, and R9) at the active site of Glucosamine-6P synthase (PDB ID: 4AMV) along with their 2D interactions. The interacting residues of the protein are represented in the yellow color stick model and chalcones (R6, R1, R5 and R9) in the green color stick model. Conventional hydrogen bonds are represented in green, and non-covalent interactions are represented in pink.

4. Conclusion

The study highlights the antibacterial, antifungal, and molecular docking study of chalcones (R1 to R20), demonstrating their potential as antimicrobial agents. Among the synthesized chalcones, R1, R5, R6, and R18 exhibited the most potent antibacterial activity with MIC values of 32 µg/mL, attributed to the presence of electron-withdrawing groups like dichloro, nitro, and difluoro moieties. Similarly, R1, R3, and R18 displayed significant antifungal activity, with MIC values of 16 µg/mL, indicating the dual antimicrobial potency of R1 and R18. Structure-activity relationship (SAR) analysis revealed that electron-withdrawing and electron-releasing substituent's on the phenyl ring significantly

modulated antimicrobial activity, suggesting that further structural modifications could enhance potency. Protein quality evaluation of PDB: 4AMV confirmed its suitability for docking studies, with 92.7% of residues in favored regions and high-quality assessment scores. Docking studies identified R6 as the top-performing ligand with the highest binding affinity (-8.4 kcal/mol), forming three hydrogen bonds and multiple hydrophobic interactions within the active site of PDB: 4AMV. R1, R5, and R9 also showed competitive binding affinities (-8.2 to -8.0 kcal/mol), highlighting their potential as ciprofloxacin alternatives. These ligands' strong binding affinities and interaction profiles underscore their potential as lead compounds for antimicrobial drug development, warranting further in-depth investigations.

Acknowledgment

The authors thanked Prof. Y. Srinivasa Rao, Principal of Vignan Institute of Pharmaceutical Technology and Lavu Educational Society, for providing the facilities needed for this study.

Conflict of interest

The authors disclose no conflicts of interest.

Using artificial intelligence chatbots

There was no use of artificial intelligence in the making of this article.

References

1. Richard JF, Yitzhak T. Antibiotics and bacterial resistance in the 21st century. Perspect Med Chem. 2014; 6:S14459.
2. Halling-Sørensen B. Inhibition of aerobic growth and nitrification of bacteria in sewage sludge by antibacterial agents. Arch Environ Contam Toxicol. 2001; 40:451–60.
3. Harish C, Parul B, Archana Y, Babita P, Abhay PM, Anant RN. Antimicrobial resistance and the alternative resources with special emphasis on plant-based antimicrobials—a review. Plants. 2017; 6:16.
4. Francesca P, Patrizio P, Annalisa P. Antimicrobial resistance: A global multifaceted phenomenon. Pathog Glob Health. 2015; 109:309–18.
5. Bingyun L, Thomas JW. Bacteria antibiotic resistance: New challenges and opportunities for implant-associated orthopedic infections. J Orthop Res. 2018; 36:22–32.
6. U.S. Food and Drug Administration. Novel Drug Approvals for 2017. Available from: https://www.fda.gov/drugs/new-drugs-fda-cdersnew-molecular-entities-and-new-therapeutic-biological-products/novel-drug-approvals-2017
7. U.S. Food and Drug Administration. Novel Drug Approvals for 2018. Available from: https://www.fda.gov/drugs/new-drugs-fda-cdersnew-molecular-entities-and-new-therapeutic-biological-products/novel-drug-approvals-2018
8. Wang W, Sun Q. Novel targeted drugs approved by the NMPA and FDA in 2019. Signal Transduct Target Ther. 2020;5(65):1–4.
9. Nurken B, Mohamad A. An overview of drug discovery and development. Future Med Chem. 2020; 12:939–47.
10. Alam MS, Rahman SM, Lee DU. Synthesis, biological evaluation, quantitative-SAR, and docking studies of novel chalcone derivatives as antibacterial and antioxidant agents. Chem Pap. 2015; 69(8):1118–29. https://doi.org/10.1515/chempap-2015-0113
11. Singh P, Anand A, Kumar V. Recent developments in biological activities of chalcones: A mini review. *Eur J Med Chem*. 2014; 85:758–77. DOI:10.1016/j.ejmech.2014.08.033.
12. Wadleigh RW, Yu SJ. Glutathione transferase activity of fall armyworm larvae toward α, β-unsaturated carbonyl allelochemicals and its induction by allelochemicals. *Insect Biochem*. 1987; 17(5):759–64. DOI: 10.1016/0020-1790(87)90046-1.
13. Karthikeyan C, Narayana Moorthy NSH, Ramasamy S, Vanam U, Manivannan E, Karunagaran D, et al. Advances in chalcones with anticancer activities. *Recent Pat Anticancer Drug Discov*. 2014; 10(1):97–115. DOI: 10.2174/1574892809666140819153902.
14. Dhar K, Saxena A, Kumar S, Sapra S, Sweety, Nepali K, et al. Synthesis and biological evaluation of chalcones having heterosubstituent(s). *Indian J Pharm Sci*. 2010; 72(6):801. DOI:10.4103/0250-474X.84602.
15. Ninomiya M, Koketsu M. In: Ramawat KG, editor. *Natural Products*. Berlin: Springer Verlag; 2013.
16. Okolo EN, Ugwu DI, Ezema BE, Ndefo JC, Eze FU, Ezema CG, et al. New chalcone derivatives as potential antimicrobial and antioxidant agents. *Sci Rep*. 2021; 11:21871. DOI: 10.1038/s41598-021-01292-5.
17. Henry EJ, Bird SJ, Gowland P, Collins M, Cassella JP. Ferrocenyl chalcone derivatives as possible antimicrobial agents. *J Antibiot*. 2020; 73(5):299–308. DOI: 10.1038/s41429-020-0280-y.
18. Benouda H, Bouchal B, Challioui A, Oulmidi A, Harit T, Malek F, et al. Synthesis of a series of chalcones and related flavones and evaluation of their antibacterial and antifungal activities. *Lett Drug Des Discov*. 2018; 16(1):93–100. DOI: 10.2174/1570180815666180404130430.
19. ur Rashid H, Xu Y, Ahmad N, Muhammad Y, Wang L. Promising anti-inflammatory effects of chalcones via inhibition of cyclooxygenase, prostaglandin E2, inducible NO synthase and nuclear factor KB activities. *Bioorg Chem*. 2019; 87:335–65. DOI:10.1016/j.bioorg.2019.03.033.
20. Nurkenov O, Ibraev M, Schepetkin I, Khlebnikov A, Seilkhanov T, Arinova A, et al. Synthesis, structure, and anti-inflammatory activity of functionally substituted chalcones and their derivatives. *Russ J Gen Chem*. 2019;89(7):1360–7. DOI: 10.1134/S1070363219070028.

21. Ibrahim TS, Moustafa AH, Almalki AJ, Allam RM, Althagafi A, Md S, et al. Novel chalcone/aryl carboximidamide hybrids as potent anti-inflammatory agents via inhibition of prostaglandin E2 and inducible NO synthase activities: design, synthesis, molecular docking studies and ADMET prediction. *J Enzyme Inhib Med Chem*. 2021; 36(1):1067–78. DOI:10.1080/14756366.2021.1929201.
22. Lakshminarayanan B, Kannappan N, Subburaju T. Synthesis and biological evaluation of novel chalcones with methanesulfonyl end as potent analgesic and anti-inflammatory agents. *Int J Pharm Res Biosci*. 2020;11(10):4974–81. DOI:10.13040/IJPSR.0975-8232.11 (10).4974-81.
23. Higgs J, Wasowski C, Marcos A, Jukič M, Paván CH, Gobec S, et al. Chalcone derivatives: synthesis, in vitro and in vivo evaluation of their anti-anxiety, anti-depression and analgesic effects. *Heliyon*. 2019; 5(3):e01376. DOI:10.1016/j.heliyon.2019.e01376.
24. Murtaza S, Mir KZ, Tatheer A, Ullah RS. Synthesis and evaluation of chalcone and its derivatives as potential anticholinergic agents. *Lett Drug Des Discov*. 2019; 16(3):322–32. DOI: 10.2174/1570180815666180523085436.
25. Fakhrudin N, Pertiwi KK, Takubessi MI, Susiani EF, Nurrochmad A, Widyarini S, et al. A geranylated chalcone with antiplatelet activity from the leaves of breadfruit (*Artocarpus altilis*). *Pharmacia*. 2020;67:173. DOI:10.3897/pharmacia.67.e56788.
26. Choudhary AN, Kumar A, Juy V. Design, synthesis and evaluation of chalcone derivatives as anti-inflammatory, antioxidant and antiulcer agents. *Lett Drug Des Discov*. 2012; 9(5):479–88. DOI: 10.2174/157018012800389368.
27. Bale AT, Salar U, Khan KM, Chigurupati S, Fasina T, Ali F, et al. Chalcones and bis-chalcone analogs as DPPH and ABTS radical scavengers. *Lett Drug Des Discov*. 2021; 18(3):249–57. DOI: 10.2174/1570180817999201001155032.
28. Al Zahrani NA, El-Shishtawy RM, Elaasser MM, Asiri AM. Synthesis of novel chalcone-based phenothiazine derivatives as antioxidant and anticancer agents. *Molecules*. 2020; 25(19):4566. DOI: 10.3390/molecules25194566.
29. Qin HL, Zhang ZW, Lekkala R, Alsulami H, Rakesh K. Chalcone hybrids as privileged scaffolds in antimalarial drug discovery: a key review. *Eur J Med Chem*. 2020; 193:112215. DOI:10.1016/j.ejmech.2020.112215.
30. Ouyang Y, Li J, Chen X, Fu X, Sun S, Wu Q. Chalcone derivatives: role in anticancer therapy. *Biomolecules*. 2021;11(6):894. DOI: 10.3390/biom11060894.
31. Čižmáriková M, Takáč P, Spengler G, Kincses A, Nové M, Vilková M, et al. New chalcone derivative inhibits ABCB1 in multidrug-resistant T-cell lymphoma and colon adenocarcinoma cells. *Anticancer Res*. 2019;39(12):6499–505. DOI:10.21873/anticanres.13864.
32. Fu Y, Liu D, Zeng H, Ren X, Song B, Hu D, et al. New chalcone derivatives: Synthesis, antiviral activity and mechanism of action. *RSC Adv*. 2020;10(41):24483–90. DOI: 10.1039/D0RA03684F.
33. Alsafi MA, Hughes DL, Said MA. First COVID-19 molecular docking with a chalcone-based compound: synthesis, single-crystal structure and Hirshfeld surface analysis study. *Acta Crystallogr Sect C Struct Chem*. 2020;76(12):1043–50. doi:10.1107/S2053229620014217.
34. Duran N, Polat MF, Aktas DA, Alagoz MA, Ay E, Cimen F, et al. New chalcone derivatives as effective against SARS-CoV-2 agent. *Int J Clin Pract*. 2021; 75:e14846. doi:10.1111/ijcp.14846.
35. Kalirajan R. Activity of some novel chalcone substituted 9-anilinoacridines against coronavirus (COVID-19): a computational approach. *Coronaviruses*. 2020; 1:13–22. DOI: 10.2174/2666796701999200625210746.
36. Escrivani DO, Charlton RL, Caruso MB, Burle-Caldas GA, Borsodi MP, Zingali RB, et al. Chalcones identify cTXNPx as a potential antileishmanial drug target. *PLoS Negl Trop Dis*. 2021; 15(11):e0009951. doi:10.1371/journal.pntd.0009951.
37. Welday Kahssay S, Hailu GS, Taye Desta K. Design, synthesis, characterization and in vivo antidiabetic activity evaluation of some chalcone derivatives. *Drug Des Devel Ther*. 2021; 15:3119–29. DOI:10.2147/DDDT.S316185.
38. Jain A, Jain D. Synthesis, characterization and biological evaluation of some new heterocyclic derivatives of chalcone as antihyperglycemic agents. *Int J Pharm Sci Res*. 2019; 10(12):5700–6. DOI:10.13040/IJPSR.0975-8232.10 (12).5700-06.
39. Bhoj P, Togre N, Bahekar S, Goswami K, Chandak H, Patil M. Immunomodulatory activity of sulfonamide chalcone compounds in mice infected with filarial parasite, *Brugia malayi*. *Indian J Clin Biochem*. 2019; 34(2):225–9. DOI: 10.1007/s12291-017-0727-5.
40. Lee JS, Bukhari SNA, Fauzi NM. Effects of chalcone derivatives on players of the immune system. *Drug Des Devel Ther*. 2015; 9:4761. DOI:10.2147/DDDT.S86242.
41. Reddy MR, Aidhen IS, Reddy UA, Reddy GB, Ingle K, Mukhopadhyay S. Synthesis of 4-C-β-D-glucosylated isoliquiritigenin and analogues for aldose reductase inhibition studies. *Eur J Org Chem*. 2019; 2019(24):3937–48. DOI:10.1002/ejoc.201900413.
42. Shah U, Patel S, Patel M, Gandhi K, Patel A. Identification of chalcone derivatives as putative non-steroidal aromatase inhibitors potentially useful against breast cancer by molecular docking and ADME prediction. *Indian J Chem*. 2020; B59:283–9.
43. Aljohani G, Al-Sheikh Ali A, Alraqa SY, Itri Amran S, Basar N. Synthesis, molecular docking and biochemical analysis of aminoalkylated naphthalene-based chalcones as acetylcholinesterase inhibitors. *J Taibah Univ Sci*. 2021; 15(1):781–97. DOI:10.1080/16583655.2021.2005921.
44. Bui TH, Nguyen NT, Dang PH, Nguyen HX, Nguyen MTT. Design and synthesis of chalcone derivatives as potential non-purine xanthine oxidase inhibitors. *SpringerPlus*.2016; 5(1):1789. DOI: 10.1186/s40064-016-3485-6.
45. Claisen L, Claparede B. Condensationen von Ketonen mit Aldehyden. *Ber Dtsch Chem Ges*. 1881; 14:2463.

46. Shaik AB, Bhandare RR, Nissankararao S, Edis Z, Tangirala NR, Shahanaaz S, et al. Design, facile synthesis and characterization of dichloro substituted chalcones and dihydropyrazole derivatives for their antifungal, antitubercular and antiproliferative activities. *Molecules*. 2020; 25:3188. DOI: 10.3390/molecules25143188.
47. Dassault Systèmes . BIOVIA Discovery Studio Visualizr; Dassault Systèmes: San Diego, 2020.
48. Rathod S, Shinde K, Porlekar J, Choudhari P, Dhavale R, Mahuli D, et al. Computational Exploration of Anticancer Potential of Flavonoids against Cyclin-Dependent Kinase 8: An In Silico Molecular Docking and Dynamic Approach. ACS Omega. 2022 Dec 21;8(1):391-409. DOI: 10.1021/acsomega.2c04837. PMID: 36643495; PMCID: PMC9835631.
49. Dym O, Eisenberg D, Yeates TO. Detection of errors in protein models. In: International Tables for Crystallography Volume F: Crystallography of Biological Macromolecules. Springer; 2006.
50. Bhowmik D, Nandi R, Prakash A, Kumar D. Evaluation of flavonoids as 2019-NCoV cell entry inhibitors through molecular docking and pharmacological analysis. Heliyon. 2021; 7:e06515. https://doi.org/10.1016/j.heliyon.2021.e06515.
51. Wiederstein M, Sippl MJ. ProSA-Web: Interactive web service for the recognition of errors in three-dimensional structures of proteins. Nucleic Acids Res. 2007; 35:W407–W410. https://doi.org/10.1093/nar/gkm290.
52. Laskowski RA, Macarthur MW, Thornton JM. PROCHECK: A program to check the stereochemical quality of protein structures. J Appl Cryst. 1993; 26:283–91. https://doi.org/10.1107/S0021889892009944.
53. Tian et al. Nucleic Acids Res. 2018. PMID: 29860391. https://doi.org/10.1093/nar/gky473.
54. Eberhardt J, Santos-Martins D, Tillack AF, Forli S. AutoDock Vina 1.2.0: New docking methods, expanded force field, and Python bindings. J Chem Inf Model. 2021;61:3891–8. https://doi.org/10.1021/acs.jcim.1c00203.
55. Stanzione F, Giangreco I, Cole JC. Use of molecular docking computational tools in drug discovery. Prog Med Chem. 2021; 60:273–343. https://doi.org/10.1016/bs.pmch.2021.01.004.
56. Ikwu FA, Isyaku Y, Obadawo BS, Lawal HA, Ajibowu SA. In silico design and molecular docking study of CDK2 inhibitors with potent cytotoxic activity against HCT116 colorectal cancer cell line. J Genet Eng Biotechnol. 2020;18:51. https://doi.org/10.1186/s43141-020-000662.
57. Dallakyan S, Olson AJ. Small-molecule library screening by docking with PyRx. Methods Mol Biol. 2015; 1263:243–50. https://doi.org/10.1007/978-1-4939-2269-7_19.
58. Vanangamudi G, Subramanian M, Jayanthi P, Arulkumaran R, Kamalakkannan D, Thirunarayanan G. IR and NMR spectral studies of some 2-hydroxy-1-naphthylchalcones: Assessment of substituent effects. Arab J Chem. 2011. doi:10.1016/j.arabjc.2011.07.019.
59. Mala V, Sathiyamoorthi K, Sakthinathan SP, Kamalakkannan D, Suresh R, Vanangamudi G, Thirunarayanan G. Solvent-free synthesis, spectral correlations and antimicrobial activities of some 3,4-dimethoxychalcones. Q-Science Connect. 2013. DOI:10.5339/connect.2013.7.
60. Opletalova V, Hartl J, Palat K Jr, Patel A. Conformational analysis of 2-hydroxy-2′,5′-diazachalcones. J Pharm Biomed Anal. 2000; 23:55–59.
61. Rao MLN, Houjou H, Hiratani K. Novel synthesis of macrocycles with chalcone moieties through mixed aldol reaction. Tetrahedron Lett. 2001; 42:8351–8355.
62. Jung YJ, Son KI, Oh YE, Noh DY. Ferrocenyl chalcones containing anthracenyl group: Synthesis, X-ray crystal structures and electrochemical properties.
63. Immadisetty SK, Saravanan G, Vamsi J, et al. Synthesis, characterization and antimicrobial activity of some novel N-((1H-benzoimidazol-1-yl)methyl)-4-(1-phenyl-5-substituted-4,5-dihydro-1H-pyrazol-3-yl)benzenamine derivatives. Pharmacognosy Res. 2014; 6(1):40–49.
64. Kucerova-Chlupacova M, Kunes J, Buchta V, et al. Novel halogenated pyrazine-based chalcones as potential antimicrobial agents. Molecules. 2016; 21(11):1421.
65. da Silva DL, de Souza MV, Frugulhetti IC, et al. Antimicrobial and cytotoxicity potential of acetamido, amino and nitrochalcones. Planta Med. 2012; 78(18):1863–1868.
66. Zhan W, Zhou R, Mao P, et al. Synthesis, antifungal activity and mechanism of action of novel chalcone derivatives containing 1,2,4-triazolo-[3,4-b]-1,3,4-thiadiazole. Mol Divers. 2024; 28(2):461–474.
67. Marques BC, Santos MB, Anselmo DB, et al. Methoxychalcones: effect of methoxyl group on the antifungal, antibacterial, and antiproliferative activities. Med Chem. 2020; 16(7):881–891.